Assessing the transport rate of hyperpolarized pyruvate and lactate from the intra- to the extracellular space

Assessment of the exchange rate of hyperpolarized pyruvate and lactate across the cellular membrane.

F. Reineri, V. Daniele, S. Aime

[1]*University of Torino, Dep.Molecular Biotechnology and Health Sciences, Torino Italy;*

Key words: hyperpolarization, Dynamic Nuclear Polarization, pyruvate, Gd(III) complexes, relaxometry, monocarboxylate transporter.

Abbreviations: DNP: Dynamic Nuclear Polarization; MCT: Monocarboxylate transporters; Gd-DO3A : Gd-tetraazacyclododecane tri-acetic acid; LDH: Lactate Dehydrogenase.

Abstract

The use of [1-^{13}C] pyruvate hyperpolarized by means of DNP provides direct access to metabolic transformations of this metabolite *in vivo* and in cells cultures. Differentiation of the intra and extracellular metabolite component in the 13C NMR spectra is not straightforward and, in order to obtain information about the activity of monocarboxylate transporter proteins (MCT) some . The purpose of this study is to investigate the rate of pyruvate and lactate transport through the cellular membrane. This is pursued by means of the heptacoordinated Gd-DO3A complex, that allows a dramatic decrease of the relaxation time of the ^{13}C-carboxylate resonances of pyruvate and lactate. When Gd-DO3A is added to a MCF-7 cellular culture, that previously received a dose of hyperpolarized [1-^{13}C] pyruvate, a sudden "quenching" of the extracellular pyruvate and lactate signal takes place. From the analysis of the decay curves of the ^{13}C-carboxylate resonances of pyruvate and lactate it is possible to extract useful information about the exchange rate of the two metabolites across the cellular membrane. In particular it is found that the rate of pyruvate transport from the intra to the extracellular compartment is null whereas that of lactate is rather high (about 30 fmol cell^{-1} min^{-1}). The herein reported method is non-destructive and can be translated to *in vivo* studies. It opens the way for the use of hyperpolarized pyruvate to assess altered activity of carboxylate transporter proteins that may occur in pathological conditions.

Introduction

Direct access to metabolic processes *in vivo* was made possible by the introduction of the DNP-dissolution technique that enables an outstandingly high signal enhancement of NMR resonances in respect to their intensities at thermal equilibrium (1). Currently, the main application of this technique deals with ^{13}C-labelled pyruvate. The use of hyperpolarized pyruvate as a reporter of cellular metabolism represents a break-through in the field of diagnosis and therapeutic monitoring of tumours (2,3). Part of the hyperpolarized pyruvate administered *in vivo* or in cells cultures enters the cells and transforms to lactate. Enzymatic activity is related to The anaerobic transformation of pyruvate into lactate is up-regulated in

cancer cells, therefore the relative amount of detected hyperpolarized lactate can be taken as a readout of the occurrence of an altered metabolic pathway.

The intracellular pyruvate and lactate concentrations are related to the activity of membrane transporter proteins, i.e. they are determined by the exchange rate between the intra and extracellular compartments mediated by the monocarboxylate transporters (MCT) (4). This feature is well known and it has also been shown that inhibition of MCT affects cancer cells proliferation (5). However its real time quantification is not straightforward and we have deemed of interest to search for a method that allows to determine the rate of metabolites transport through the cellular membrane by using hyperpolarized pyruvate.

Actually, two experimental approaches have already been tested to get this goal. The method reported by Harris (6) consists of incubating a cells culture with pyruvate and, after a given delay time, proceeding with a quick washing out of the incubating medium. By this procedure, the extracellular metabolites are removed and only the intracellular pyruvate and its metabolites are observed. According to this study, the membrane transport of pyruvate is the rate limiting step in the formation of lactate.

A different approach to assess the role of MCT activity on the pyruvate to lactate conversion rate was applied by Witney et al (7). In this case, the pyruvate to lactate transformation rate was measured in both intact and lysed cells and, having observed that in the cells lysate the metabolic conversion is only a little faster than in intact cells, it was concluded that MCT transport is not rate limiting for lactate production.

Moreover, other studies address the topic of compartmentalization of metabolites, allowing to distinguish between the amounts of intra and extracellular pyruvate and lactate. These studies rely on the different diffusion coefficients of small molecules in intra and extracellular spaces and have been carried out either *in vivo* (8,9) and in cells cultures (10). However, these studies do not provide information about rate of transport through cellular membrane.

The design of the herein reported study relies on the effect of a Gd-based paramagnetic agent on the relaxation of the hyperpolarized signals. These paramagnetic metal complexes cannot enter the cells and the thickness of cell membranes (~ 3 nm) protects intracellular compounds

from their relaxation effects. On the contrary, the polarization of the extracellular molecules may be strongly affected or even instantaneously "quenched" upon their interaction with the paramagnetic species. As a consequence, the observed T_1-kinetics of the metabolites can be ascribed only to intracellular processes and/or to the exchange across the cellular membrane.

The use of Gd-based contrast agents for "quenching" the ^{13}C polarization of the metabolites in the extracellular compartment has already been proposed (11, 12), but the observed effect was of limited entity. In fact, in these studies commercial contrast agents have been employed (Omniscan, Magnevist, Dotarem, Gadovist), for which only an outer sphere relaxation mechanism could be operative. Herein we show that a much higher efficiency in destroying the hyperpolarization in the extracellular compartment can be achieved by using the "coordinatively unsaturated" Gd-DO3A complex (13). The heptadentate ligand leaves two vacancies in the inner coordination sphere of the Gd(III) ion that can be occupied by donor atoms from the carboxylate moieties of pyruvate or lactate (14). Therefore this Gd(III) complex is much more efficient in enhancing the ^{13}C relaxation rates than other coordinatively saturated complexes, such as Gd-HP-DO3A or Gadodiamide, whose ability to enhance the relaxation rate of carboxyl moieties relies only on the less efficient outer sphere mechanism.

Experimental

The reversible formation of a ternary adduct between GdDO3A and the substrate of interest has been assessed by *in vitro* ^1H-NMR relaxometry. Upon titrating a 1 mM solution of Gd-DO3A with pyruvate or lactate, change in water protons relaxation rate as a function of the substrate concentration allows to obtain the respective binding affinity. Relaxation measurements have been carried out using a Stelar relaxometer operating at 0.5 T. The binding affinity constants (K_A) have been derived by applying the so-called Proton Relaxation Enhancement method (14). The effect of Gd-DO3A on the relaxation rate of ^{13}C carboxylate signals of pyruvate and lactate has been investigated. To an aqueous solution (Phosphate-Buffered Saline 30 mM) of the metabolite (10 mM) the Gd-DO3A complex has been added at two different concentrations, 0.1 mM and 1 mM. The T_1 of the ^{13}C carboxylate signals has been measured using the inversion

recovery pulse sequence on a Bruker Avance 600 MHz NMR spectrometer. The T_1 measurements have also been carried out using the complex Gd-HP-DO3A.

The "quenching" of the ^{13}C signal of substrates present in the extracellular compartment has been pursued by adding Gd-DO3A to a suspension of breast cancer cells (MCF-7) previously treated with hyperpolarized pyruvate. The cells suspension (0.5 ml aqueous buffer, $2*10^7$ cells) has been placed into a 10 mm NMR tube inside a 14.1 T magnet. The set-up for mixing of pyruvate and Gd-DO3A into the cells suspension is described in the Supplementary Material.

1-^{13}C pyruvate has been hyperpolarized at 3.3 T and 1.2 K, as previously reported (1), until about 25% polarization has been reached. The sample has been dissolved in 5 ml of phosphate buffer (40 mM) and 2 ml have been perfused to the cells, resulting in a pyruvate concentration of 3 mM in the cells suspension. After 10 s a solution of Gd-DO3A has been added, resulting in a concentration of 0.3 mM of the paramagnetic complex. A series of 1D spectra (20° pulses, 2 seconds delay) covering the full experiment time has been acquired.

Fitting of the experimental data has been carried out using the equations described in the Discussion section and in the Supplementary Material.

Results

The binding affinity between the metal complex Gd-DO3A and the substrates pyruvate and lactate has been obtained by means of the Proton Relaxation Enhancement method. This relies on the fact that coordination of pyruvate or lactate to the Gd(III) centre implies the replacement of one or two water molecules from the inner coordination sphere of the paramagnetic metal ion, with a consequent decrease of the relaxation rate of water protons. The water protons relaxation rates obtained at increasing concentrations of metabolites are reported in Figure 1. From the analysis of these curves, it is possible to estimate a binding affinity constant K_A of 150 ± 10 M^{-1} for lactate, as already reported by Terreno et al. (14). On the other hand, for pyruvate, the K_A results almost an order of magnitude lower, i.e. 25.9 ± 2.0 M^{-1}. This difference in the binding affinity may be accounted for by the fact that lactate

acts as a bi-dentate ligand (14), while pyruvate seems to coordinate the metal centre only through the carboxylic moiety (15).

The binding affinities of the two substrates to Gd-DO3A are sufficiently high to generate a dramatic effect on the relaxation rate of the ^{13}C carboxylate signal of pyruvate and lactate. When the concentration of Gd-DO3A is 1/10 of that of the metabolites, the T_1 of the ^{13}C carboxylate signal is about 40 ms for both (Table 1). Therefore one can conclude that the hyperpolarized signal of these metabolites is completely cancelled in 2 s, that is the delay between the acquisition of successive data points in our experiments. On this basis, we have considered the hyperpolarized signal instantaneously quenched.

When the concentration of Gd-DO3A is decreased to 1/100 of that of the metabolites, its effect on T_1s is about one order of magnitude lower.

When the coordinatively saturated complex Gd-HP-DO3A is used, the measured T_1s are much longer, yielding for instance almost 3 s for the ^{13}C carboxylate signal of pyruvate when the ratio between the metal complex and the substrate is 1/10.

Upon the addition of Gd-DO3A to the cells suspension, the hyperpolarized signals of pyruvate and lactate decay abruptly (Figure 2), because the extracellular hyperpolarized signal is completely cancelled in the time space between two successive acquisitions and the remaining signal is due only to the intracellular component. Thus, the amount of intracellular polarized pyruvate resulted to be 0.55±0.15% of the total administered polarized pyruvate, corresponding to about $41.2\pm11*10^{-9}$ mol of intracellular pyruvate (about 2 fmol/cell). The amount of intracellular lactate is slightly lower than that of pyruvate ($28.8*10^{-9}$ mol, 1.4 fmol/cel).

The pulse corrected decay time constants after Gd-DO3A addition are 6.4 ± 0.3 s and 7.5 ± 0.2 s for pyruvate and lactate, respectively (Figure 3). They are obtained from fitting of the experimental points by monoexponential decay .

Discussion

In order to find how the pyruvate and lactate signal decay after Gd addition can be taken as a readout of metabolites transport rate through the cellular membrane, several factors have to be considered (Figure 4): the intracellular T_1 of the two metabolites, their mutual conversion catalized by lactate dehydrogenase (LDH) and their transport from intra to extracellular space.

The differential equations that describe these processes are the following:

$$\frac{dPy_{Int}}{dt} = - k_{P\text{-}L} \cdot Py_{Int} + k_{L\text{-}P} \cdot Lac_{Int} - k_{PyExt} \cdot Py_{Int} - \frac{1}{T_1^{PyInt}} Py_{Int} \qquad (1)$$

$$\frac{dLac_{Int}}{dt} = k_{P\text{-}L} \cdot Py_{Int} - k_{L\text{-}P} \cdot Lac_{Int} - k_{LacExt} \cdot Lac_{Int} - \frac{1}{T_1^{LacInt}} Lac_{Int} \qquad (2)$$

where $k_{P\text{-}L}$ and $k_{L\text{-}P}$ are the kinetic constants of pyruvate to lactate mutual conversion catalyzed by LDH, k_{PyExt} and k_{LacExt} are the kinetic constants for metabolites transport to the extracellular space and the T_1s refer to the relaxation times of intracellular pyruvate and lactate.

As far as the intracellular relaxation times of metabolites are concerned, their values are affected by the microviscosity of cell cytoplasm and transient interactions with slowly moving macromolecules (16). It was reported that these two contributions reduce the rotational mobility of a small molecule to about 60% of its value in neat water. Having T_1 values in buffer solution of 43 s and 35 s for pyruvate and lactate respectively, the intracellular T_1s can be estimated to be about 26 s and 21 s. Because pyruvate and lactate are rapidly exchanging, an average T_1 can be considered. Furthermore, an indirect measurement of intracellular T_1 of pyruvate and lactate has recently been reported upon the administration of hyperpolarized glucose to perfused MCF-7 cells (17). This yielded an average T_1 of 16 s for both metabolites. In our fittings both sets of T_1 values have been used.

Concerning the intracellular reactions catalyzed by LDH, both kinetic constants, k_{PL} and k_{LP}, should be considered in our equations because it was shown that the reaction is an equilibrium (18). However, due to the huge concentration of hyperpolarized pyruvate with respect to the concentration of pyruvate at physiological conditions, a net conversion of pyruvate into lactate is observed. Moreover, while almost all pyruvate is hyperpolarized, most of lactate is not, therefore the back conversion rate of lactate to pyruvate results less important in determining

the actual intensities of the hyperpolarized signals of the two metabolites. Therefore, in our fitting model, we neglect k_{LP} and only use the kinetic constant k'_{PL} (where the "prime" label informs that net pyruvate to lactate transformation is considered). Then equations 1 and 2 reduce to

$$\frac{dPy_{Int}}{dt} = - k'_{P\text{-}L} \cdot Py_{Int} - k_{PyExt} \cdot Py_{Int} - \frac{1}{T_1^{PyInt}} Py_{Int} \qquad (3)$$

$$\frac{dLac_{Int}}{dt} = k'_{P\text{-}L} \cdot Py_{Int} - k_{LacExt} \cdot Lac_{Int} - \frac{1}{T_1^{LacInt}} Lac_{Int} \qquad (4)$$

Next, one has to consider that, upon the addition of the paramagnetic complex, a large pool of non-polarized metabolites (pyruvate and lactate) is formed in the extracellular compartment. Such extracellular metabolites, and mainly pyruvate, take part to the metabolic transformations, but are not detected in the NMR spectra as the observed signal is only due to the hyperpolarized molecules. As a consequence, the apparent reaction rates are gradually reduced as the metabolic processes proceed. In order to account for this effect, Py_{Int} and Lac_{Int} in the equations have to be modified as follows:

$$Py_{Int} = PyP_{Int} = \frac{PyP_{Int}}{PyT_{Int}} PyT_{Int} = X_{PyPInt}(t) PyT_{Int} \qquad (5)$$

$$Lac_{Int} = LacP_{Int} = \frac{LacP_{Int}}{LacT_{Int}} LacT_{Int} = X_{LacPInt}(t) LacT_{Int} \qquad (6)$$

Where i) X_{PyPInt} and $X_{LacPInt}$ are the polarized intracellular molar fractions (PyP_{Int}/PyT_{Int} and $LacP_{Int}/LacT_{Int}$); ii) PyT_{Int} and $LacT_{Int}$ are the total amounts of intracellular pyruvate and lactate respectively. It can be assumed that the total amount of each metabolite (PyT_{Int} and $LacT_{Int}$) is constant, while the polarized part gradually tends to zero because it is no longer supplied from the extracelluar compartment. Therefore, before the Gd addition, all the intracellular pyruvate is polarized (the T_1 decay is already accounted for in the equations) and $X_{PyPInt} = X_{LacPInt} = 1$, but, after Gd administration, all the extracellular signal is cancelled, X_{PyPInt} and $X_{LacPInt}$ become time dependent and tend to zero. The equations 3 and 4 become

$$\frac{dPy_{Int}}{dt} = - k'_{P\text{-}L} \cdot X_{PyPInt}(t) \cdot PyT_{Int} - k_{PyExt} \cdot X_{PyPInt}(t) \cdot PyT_{Int} - \frac{1}{T_1^{PyInt}} Py_{Int} \qquad (7)$$

$$\frac{dLac_{Int}}{dt} = k'_{P\text{-}L} \cdot X_{PyPInt}(t) \cdot PyT_{Int} - k_{LacExt} \cdot X_{acPInt}(t) \cdot LacT_{Int} - \frac{1}{T_1^{LacInt}} Lac_{Int} \quad (8)$$

The experimental curves of pyruvate and lactate signal intensities have then been fitted to these equations. Pyruvate and lactate time dependence is simulated by means of an on-purpose written function (Matlab 7.0) and the experimental data are interpolated to the calculated values (see Supplementary material). The rate of pyruvate and lactate transport from intra to extracellular space (k_{LacExt}, k_{PyrExt}) and the rate of intracellular pyruvate to lactate net conversion (k_{PL}) are obtained, as reported in Table 2.

The conversion rate of pyruvate to lactate before the addition of the paramagnetic complex has also been determined by interpolating the experimental data acquired before Gd addition with the values calculated from the following equations (see Supplementary Material).

$$\frac{dPy}{dt} = -k_{PL}^{0} \cdot Py - \frac{1}{T_1^{Py}} \cdot Py \quad (9)$$

$$\frac{dLac}{dt} = k_{PL}^{0} \cdot Py - \frac{1}{T_1^{Lac}} \cdot Lac \quad (10).$$

In this case, intra and extracellular compartments cannot be distinguished and the system can be described by a two pools exchange model. The corresponding rate of pyruvate to lactate transformation is determined by two coupled events, i.e. the transport of pyruvate into the cells and the intracellular metabolic transformation. The value estimated for this overall rate of transformation of pyruvate into lactate (v_{PL}^{0}) is reported in Table 3.

From the kinetic constants reported in table 2, it can be observed that experimental data are well interpolated using a rather large range of pyruvate to lactate net conversion rates, as well as quite different rates of transport of pyruvate and lactate from intra to extracellular compartment. However, from the comparison between the intracellular rate of pyruvate to lactate transformation, obtained after addition of the paramagnetic complex (v'_{PL}), and the overall rate of this metabolic process, obtained before Gd addition (v_{PL}^{0}), it is obvious to assume that the intracellular rate of pyruvate to lactate conversion cannot be lower than that obtained using the two pools model. Therefore, by ruling out all the v'_{PL} rates lower than v^{0}_{PL}, one can conclude, from table 2, that the rate of pyruvate transport to extracellular space (k_{PyExt}) is almost zero. This is consistent with the fact that pyruvate is a fuel for cells and, when

internalized, it is quickly transformed into lactate. Furthermore, since the intracellular rate of pyruvate to lactate conversion is only slightly higher than the overall rate v^0_{PL}, obtained with the two pools model, we can deduce that the rate of pyruvate internalization, i.e. of transport from the extra to the intracellular compartment, is not rate limiting in the metabolic conversion of pyruvate to lactate. This result is in accordance with what reported by Witney *et al.* (7), who measured pyruvate into lactate exchange rate in intact and lysed cells, finding a small difference between the two rates.

On the contrary, the rate of lactate transport to the extracellular compartment is rather high (from 24 to 30 fmol $cell^{-1}$ min^{-1}), that is consistent with the fact that lactate is a waste product of cells. The speed of lactate transport to the extracellular space is also consistent with the amount of intracellular lactate observed immediately after the Gd-DO3A addition.

Thus, the herein reported results show that the use of the paramagnetic Gd-DO3A complex allows almost instantaneous "quenching" of the hyperpolarization of extracellular pyruvate and lactate and provide indirect information about the rates of metabolites transport through the cellular membrane. These findings open the way for the use of hypeprolarized pyruvate to assess altered activity of transport proteins (e.g. MCT) that may occur in pathological conditions and may be highly important for phenotyping tumours.

In comparison to other paramagnetic complexes that have been previously used to quench extracellular hyperpolarization (11,12), in the present case, the relaxation rate is much faster and it can be safely assumed that the signal intensities observed after Gd-DO3A addition can be ascribed to the intracellular components.

Furthermore, a simple two pools model has been developed to describe the kinetics of pyruvate and lactate hyperpolarized signals after Gd addition and the exchange rates of the metabolites through the cellular membrane are derived from interpolation of the experimental data with the simulated curves.

Importantly, the herein reported method is non-destructive and can be translated to *in vivo* studies.

Acknowledgments

Albeda Research, in particular P.R. Jensen, is gratefully acknowledged for the experimental results and fruitful discussion.

References

(1) Ardenkjær-Larsen JH, Fridlund B, Gram A, Hansson G, Hansson L, Lerche MH, Servin R, Thaning M, Golman K. Increase in signal-to-noise ratio of >10000 times in liquid state NMR. *Proc. Nat. Acad. Sci.* 2003; **100**: 10158-10163.

(2) Comment A, Merritt ME. Hyperpolarized Magnetic Resonance as a Sensitive Detector of Metabolic Function. *Biochemistry* 2014; **53**: 7333-7357.

(3) Kurhanewicz J, Vigneron DB, Brindle K, Chekmenev EY, Comment A, Cunningham CH, DeBerardinis RJ, Green GG, Leach MO, Rajan SS, Rizi RR, Ross BD, Warren WS, Malloy CR Analysis of Cancer Metabolism by Imaging Hyperpolarized Nuclei: Prospects for Translation to Clinical Research. *Neoplasia* 2011; **13**: 81–97.

(4) Halestrap AP, Price NT. The proton linked carboxylate transporters (MCT) family: structure, function and regulation. *Biochem. J.* 1999; **343**: 281-299.

(5) Diers AR, Katarzyna A. Broniowska KA, Chang CF, Neil Hogg N. Pyruvate fuels mitochondrial respiration and proliferation of breast cancer cells: effect of monocarboxylate transporter inhibition. *Biochem. J.* 2012, **444**: 561–571.

(6) Harris T, Eliyahu G, Freedman L, Degani H. Kinetics of hyperpolarized ^{13}C1-pyruvate transport and metabolism in living human breast cancer cells. *Proc. Nat. Acad. Sci.* 2009; **106**: 18131-18136.

(7) Witney TH, Kettunen M, Brindle KM. Kinetic modeling of hyperpolarized ^{13}C label exchange between pyruvate and lactate in tumor cells. *J. Biol. Chem.* 2011; **286**: 24572-24580.

(8) Larson PR, Hurd RE, Kerr AB, Pauly JM, Bok RA, Kurhanewicz J, Vigneron DB. Perfusion and diffusion sensitive ^{13}C stimulated-echo MRSI for metabolic imaging of cancer. *Magn Reson Imag*. 2013; **31**:635-42.

(9) Chen AP, Leung K, Lam W, Hurd RE, Vigneron DB, Cunningham CH. Design of spectral-spatial outer volume suppression RF pulses for tissue specific metabolic characterization with hyperpolarized ^{13}C pyruvate. *J. Magn. Reson.* 2009; **200**: 344–348.

(10) Schilling F, Düwel S, Köllisch U, Durst M, Schulte RF, Glaser S J, Haase A, Otto AM, Menzel MI. Diffusion of hyperpolarized ^{13}C-metabolites in tumor cell spheroids using real-time NMR spectroscopy. *NMR Biomed.* 2013; **26**:557-68.

(11) Gabellieri C, Leach MO, Eykyn TR. Modulating the relaxivity of hyperpolarized substrates with gadolinium contrast agents. *Contrast Media Mol. Imag.* 2009; **4**:143-147.

(12) Smith MR, Peterson ET, Gordon JW, Niles DJ, Rowland IJ, Kurpad KN. Fain SB. In vivo imaging an spectroscopy of dynamic metabolism using simultaneous ^{1}H and ^{13}C MRI. *IEEE transactions on Biomed. Egineering*. 2012; **59**: 45-49.

(13) Terreno E, Botta M, Fedeli F, Mondino B, Milone L, Aime S. Enantioselective recognition between chiral α-Hydroxy−Carboxylates and

Macrocyclic Heptadentate Lanthanide(III) Chelates. *Inorg.Chem.* 2003, **42**: 4891-4897.

(14) Terreno E, Botta M, Boniforte P, Bracco C, Milone L, Modino B, Uggeri F, Aime S. A multinuclear NMR relaxometry study of Ternary adducts formed between heptadentate GdIII chelates and l-lactate. *Chem. Eur. J.* 2005; **11**: 5531-5537.

(15) Choppin GR, Cannon RE. Complexation of Lantanides by pyruvate. *Inorg. Chem.* 1980; **19**: 1889-1892

(16) Kao HP, Abney JR, Verkman AS. Determinants of the translational mobility of a small solute in cell cytoplasm. *J.Cell. Biol.* 1993; **120**: 175-184.

(17) Christensen CE, Karlsson M, Winther JR, Jensen PR, Lerche MH. Non-invasive in cell determination of free cytosolic [NAD^+]/[NADH] ratios using hyperpolarized glucose show large variation in metabolic phenotypes. *J. Biol. Chem.* 2014; **289**:2344-2352.

(18) Day SE, Kettunen MI, Gallagher FA, Hu DE, Lerche M, Wolber J, Golman K, Ardenkjaer-Larsen JH, Brindle KM. Detecting tumor response to treatment using hyperpolarized ^{13}C magnetic resonance imaging and spectroscopy. *Nat. Med.* 2007; **13**: 1382-1386.

Tables

	No Gd	Gd-DO3A (1:10)	Gd-DO3A (1:100)	Gd-HPDO3A (1:10)	Gd-HPDO3A (1:100)
T_1(Pyruvate)	43 ± 2 s	0.043 ± 0.005 s	0.44 ± 0.05 s	2.8 ± 0.3 s	16 ± 2 s
T_1(Lactate)	35 ± 2s	0.038 ± 0.004 s	0.24 ± 0.03 s	1.2 ± 0.1 s	16 ± 2 s

Table 1. T_1 values of pyruvate and lactate (10 mM) measured at 14.1 T in phosphate buffer (pH 7.3), with different ratios of the paramagnetic complexes GdDO3A and GdHP-DO3A.

k'_{PL} (s^{-1})	v'_{PL} fmol $cell^{-1}$ min^{-1}	k_{PyExt} (s^{-1})	k_{LacExt} (s^{-1})	v_{LacExt} fmol $cell^{-1}$ min^{-1}	T_1^{PyInt} T_1^{LacInt} (s)	R^2_{Py}	R^2_{Lac}
0.23±0.03*	29.0±3.7*	0*	0.27±0.03*	23.8±2.6*	16*	0.99	0.99
0.27±0.03*	34.0±3.7*	0*	0.33±0.03*	29.1±2.6*	21*	0.99	0.99
0.28±0.02	35.3±2.5	0	0.37±0.03	32.6±2.6	26	0.99	0.99
0.18±0.02	22.7±2.5	0.1	0.25±0.03	22.0±2.6	16	0.98	0.99
0.1±0.03	12.6±3.7	0.15	0.20±0.02	17.6±1.7	16	0.98	0.99

Table 2. Results of the fitting of the experimental time decay data (reported in figure 3) to the calculated values obtained by applying equations 7-8. The rate of intracellular pyruvate to lactate transformation (v'_{PL}) has been calculated multiplying the kinetic constant (k'_{PL}) by the intracellular concentration of pyruvate and dividing it by the number of cells. Intracellular concentration of pyruvate is obtained from the intensity of the polarized signal of pyruvate immediately after the Gd addition, that is 0.55% of the total pyruvate signal (41.2 ± $11*10^{-9}$ mol of intracellular polarized pyruvate, 41.25 ± $11*10^{-9}$ mol*k'_{PL} / $2*10^7$ cells = 2.1 k'_{PL} fmol/cell). In the same way, the amount of intracellular lactate has been estimated from the intensity of the lactate signal after Gd addition, that is about 70% of that of polarized pyruvate ($28.8*10^{-9}$ mol of intracellular polarized lactate). Precision of the fittings is given by the R^2 value. The asterix indicates the best values (see text).

k_{PL}^0 (s^{-1})	v_{PL}^0 (fmol $cell^{-1}$ min^{-1})	T_1^{Py} (s)	T_1^{Lac} (s)
0.00125 ± 0.00005	28.5 ± 1.5	30± 2	19.5 ± 1.5

Table 3. Results of the fitting of the experimental data of pyruvate and lactate kinetics before Gd addition to the calculated values obtained by applying equations 9 and 10. The rate of intracellular pyruvate to lactate transformation has been obtained multiplying the kinetic constant k_{PL}^0 by the total amount of pyruvate ($7.5*10^{-6}$ mol) and dividing it by the number of cells ($2*10^7$). The T_1 values have been derived from fitting.

Figures

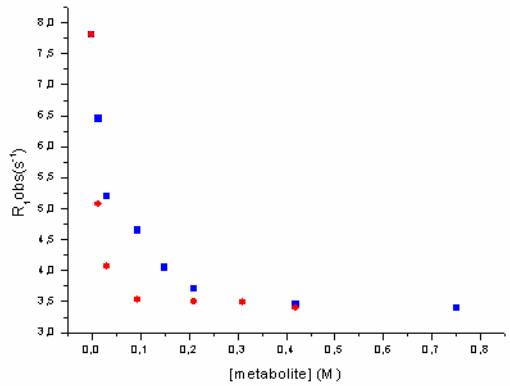

Figure 1. Water ^1H relaxation rate as a function of pyruvate (blue squares) and lactate (red dots) concentration (20 MHz, 298 K, pH 7).

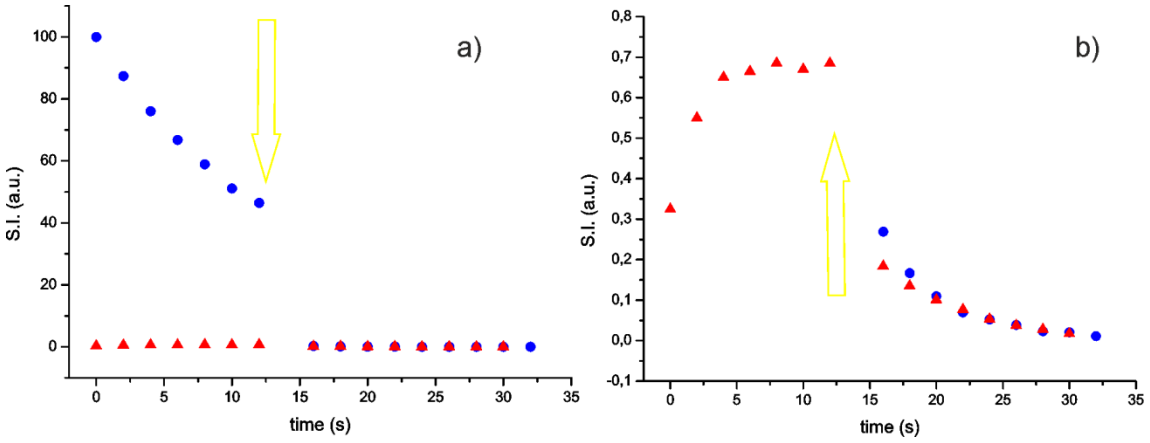

Figure 2. ^{13}C carboxyl signals of pyruvate (a) and lactate (b) before and after the addition of GdDO3A. The arrow indicates the timepoint of Gd addition; the time interval between the two sets of acquisitions corresponds to one missing spectrum (2 s).

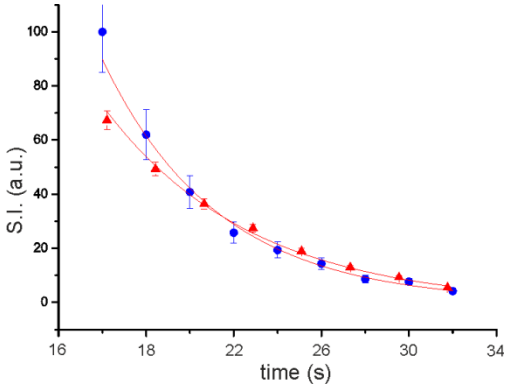

Figure 3. Time decay of [1-^{13}C]-pyruvate (blue circles) and [1-^{13}C]-lactate (red triangles) hyperpolarized signals after Gd addition.

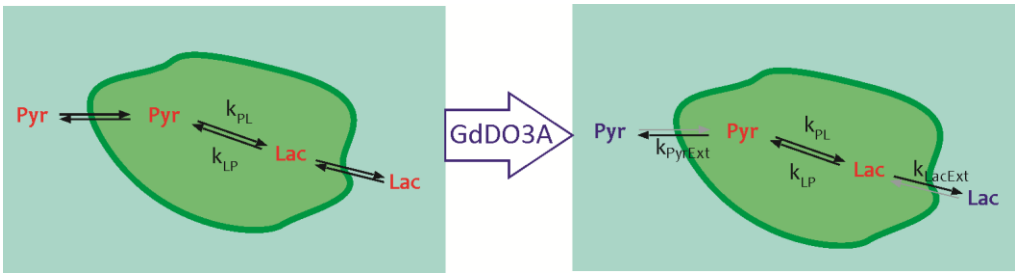

Figure 4. Schematic representation of the main steps affecting the polarization of pyruvate and lactate in a cellular suspension: before the addition of GdDO3A, both intra- and extracellular metabolites are polarized (red); upon the addition of the paramagnetic complex, the polarized signal in the extracellular compartment is instantaneously cancelled (blue).